Migration of an electrophoretic particle in a weakly inertial or viscoelastic shear flow

Aditya S. Khair * and Jason K. Kabarowski
Department of Chemical Engineering, Carnegie Mellon University, Pittsburgh, Pennsylvania 15213, USA

(Received 11 July 2019; accepted 19 February 2020; published 16 March 2020)

The motion of a spherical particle undergoing electrophoresis in weakly inertial or viscoelastic shear flow is quantified via asymptotic analysis. We are motivated by several experimental studies reporting cross-streamline migration of electrophoretic colloids in Poiseuille microchannel flow. Specifically, particles migrate in a Newtonian liquid to the center (walls) of a channel when their electrophoretic velocity is in the opposite (same) direction to (as) the flow. Here, we calculate that weak fluid inertia causes a leading-order cross-streamline lift force of magnitude $5.50\varepsilon|\zeta|a^3\rho\dot{\gamma}E^\infty/\mu$ for electrophoresis along the velocity axis of an unbounded simple shear flow, where ζ and a denote the particle zeta potential and radius, respectively; ρ, μ, and ε are the fluid density, viscosity, and permittivity, respectively; $\dot{\gamma}$ is the shear rate of the ambient flow; and E^∞ is the strength of the imposed electric field. This force acts to propel the sphere to shear streamlines that, in a frame translating with the particle, are directed reverse to the electrophoretic motion, which is consistent with the above-mentioned experiments. Other recent experiments have observed migration of electrophoretic particles in Poiseuille flow of a viscoelastic polymer solution: the migration direction is opposite to that in a Newtonian liquid. Here, we calculate a leading-order cross-streamline lift force of magnitude $7.07(1 - 3.33\Psi_2/\Psi_1)\varepsilon|\zeta|a\Psi_1\dot{\gamma}E^\infty/\mu$ for electrophoresis in simple shear flow of a second-order fluid, where Ψ_1 and Ψ_2 are the first and second normal stress coefficients, respectively. The lift is toward streamlines moving in the direction of electrophoresis for $\Psi_2/\Psi_1 < 0.3$ (a reasonable assumption for polymeric liquids, where Ψ_2 and Ψ_1 are negative and positive, respectively), which is consistent with the experiments. Finally, an estimation of the magnitude of the lift forces and associated drift velocities further suggests that the cumulative effect of weak instantaneous inertia or viscoelasticity is responsible, or at least contributes appreciably, to the observed migration.

DOI: 10.1103/PhysRevFluids.5.033702

I. INTRODUCTION

A rigid sphere translating along an ambient unidirectional flow of a Newtonian liquid does not experience a transverse, or "lift," force at zero Reynolds number. The absence thereof means that the sphere has no tendency to migrate across streamlines of the flow. Fluid inertia leads to cross-streamline migration at nonzero Reynolds number, as illustrated in the seminal work of Segré and Silberberg [1,2], who observed that neutrally buoyant spheres in a tube Poiseuille flow gather at a radial distance of 0.6 of the pipe radius from the centerline. Those experiments inspired a flurry of asymptotic analyses to calculate inertial lift forces at small particle-scale Reynolds number, for neutrally buoyant or nonneutrally buoyant spheres in bounded or unbounded flows. A good classification of such studies, in terms of the channel-scale Reynolds number of the flow, is provided

*Corresponding author: akhair@andrew.cmu.edu

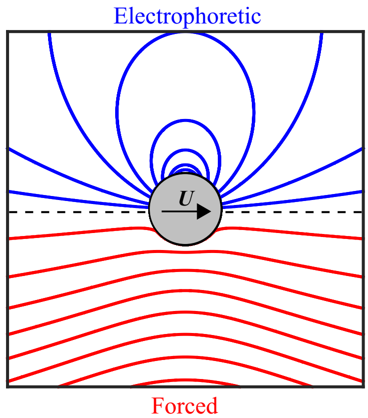

FIG. 1. Streamlines due to a sphere translating at zero Reynolds number in an otherwise quiescent fluid: the top (bottom) half shows streamlines for an electrophoretic (forced) particle. The flows are axisymmetric about the direction of translation $\boldsymbol{U}$.

in table 1 of Hogg [3]. Calculations of cross-streamline migration in viscoelastic liquids at zero Reynolds number have also been performed; see Leal [4,5] for reviews covering work in this vein up to 1980. Typically, the limit of weak viscoelasticity is analyzed [6–10], such that the fluid stress is a small departure from Newtonian. Leshansky *et al.* [11] have demonstrated tunable viscoelastic focusing of particles in microfluidic channels arising from cross-streamline forces.

Recent experiments have reported cross-streamline migration of electrically charged particles under an applied voltage and ambient flow field. For example, Kim and Yoo [12] observed that negatively charged polystyrene spheres migrate to the center of a tube as they undergo electrophoresis in the opposite direction to Poiseuille flow of a Newtonian fluid. Further experiments by this group demonstrated that inward migration also occurs in a rectangular microchannel [13]. Cevheri and Yoda [14,15], Yuan *et al.* [16], Li and Xuan [17], and Lochab *et al.* [18] showed that the direction of migration is switched by reversing the direction of the applied electric field. That is, a particle migrates to the center(walls) of the channel when its electrophoretic velocity is in the opposite(same) direction to(as) the Poiseuille flow. The switching of direction is not captured by dielectrophoretic [19,20] or electroviscous [21,22] mechanisms of cross-streamline migration, which exclusively predict repulsion from a wall. Fluid inertia has been claimed to be responsible [12,13,16]: while typical channel-scale Reynolds numbers are small, $O(0.01 - 0.1)$, it is established that inertial forces can be used to manipulate particles in microfluidic devices [23]. It has been further suggested [13,16] that theories for inertial migration of nonneutrally buoyant, or "forced," particles can rationalize this phenomenon. This is incorrect, for the following reason. At small Reynolds number the velocity disturbance due to a forced particle decays as $1/r$ (r being the distance from the particle center) at distances large compared to its characteristic linear dimension and small compared to any inertial length scale or bounding wall that screens the disturbance. In contrast, an electrophoretic particle is "force-free" in that there is no hydrodynamic force exerted on the charged particle and the diffuse (counterion) charge cloud surrounding it [24]. The size of the cloud, characterized by the Debye length, is typically much smaller than the particle size for colloids in aqueous electrolytes at milli-molar (or higher) concentration. Consequently, the velocity field around an electrophoretic particle is fundamentally different (Fig. 1): in particular, the velocity disturbance decays as $1/r^3$ at large distances for a uniformly charged particle in an unbounded fluid [25]. Recent experiments [17] have also observed migration of electrophoretic particles in shear flow of a viscoelastic polymer (PEO) solution. The migration direction is opposite to what is seen in Newtonian liquids. Predictions for migration of a forced particle in viscoelastic flow [7–10] are not applicable, again due to the different flow profile around an electrophoretic particle.

Therefore, the goal of the present work is to calculate the cross-streamline lift force on an electrophoretic particle in weakly inertial or viscoelastic shear flow. We consider a uniformly charged, spherical particle undergoing steady electrophoresis in an unbounded, steady simple shear flow. This is obviously a simplification of the relevant experiments, in which the observed migration is likely influenced by the channel walls and curvature of the Poiseuille flow. Nonetheless, our model problem will indeed predict a lift direction that is consistent with the experiments, suggesting that inertial or viscoelastic forces are relevant to the observed migration. In Sec. II we recap the electrophoresis of a particle in a Newtonian electrolyte at zero Reynolds number. In Secs. III and IV we calculate the lift force on an electrophoretic particle in weakly inertial and weakly viscoelastic (i.e., second-order fluid) shear flow, respectively. A comparison of our calculations against experimental observations is made in Sec. V. The article is concluded with a discussion in Sec. VI.

II. RECAP OF ELECTROPHORESIS AT ZERO REYNOLDS NUMBER

Consider the electrophoresis of a neutrally buoyant, uniformly charged, rigid, dielectric particle under a steady, uniform electric field in an unbounded Newtonian electrolyte at zero Reynolds number. The steady translational velocity of the particle is found from the requirement that hydrodynamic and electric forces on it sum to zero. A significant simplification occurs in the limit where the Debye length is small compared to particle size. Here, the "effective surface" enclosing the particle and the charge cloud is indistinguishable from the actual particle surface when viewed at distances comparable to the particle size. Thus, the electric stress generated by the applied field acting on the cloud is replaced by a "slip" boundary condition for the fluid velocity on the effective surface [24]. The slip velocity $\boldsymbol{v}_s = -m_e\boldsymbol{E}$, where $\boldsymbol{E}$ is the electric field at the effective surface, and $m_e = \varepsilon\zeta/\mu$ is the electro-osmotic mobility, in which ε and μ are the permittivity and viscosity of the electrolyte (assumed constant), respectively, and ζ is the zeta potential of the particle (also assumed constant). Therefore, at zero Reynolds number the fluid flow outside the effective surface, S_p, is governed by the Stokes equations

$$\mu\nabla^2\boldsymbol{v} - \nabla p = 0, \quad \nabla\cdot\boldsymbol{v} = 0, \tag{1}$$

$$\boldsymbol{v} = \boldsymbol{U} + \boldsymbol{\omega}\times\boldsymbol{r} + \boldsymbol{v}_s \;\text{ on }\; S_p, \quad \boldsymbol{v} \;\text{ and }\; p \to 0 \;\text{ as }\; |\boldsymbol{r}| \to \infty, \tag{2}$$

where $\boldsymbol{r}$ is the position vector measured from the center of the particle, and $\boldsymbol{v}$ and p are the velocity and pressure fields. The pressure is defined up to an additive constant for an incompressible fluid; thus, we state that p attenuates at large distances. The translational and angular velocities of the particle, $\boldsymbol{U}$ and $\boldsymbol{\omega}$, respectively, are determined from the conditions of zero *hydrodynamic* force ($\boldsymbol{F}^H$) and torque ($\boldsymbol{L}^H$) on S_p,

$$\boldsymbol{F}^H = \int_{S_p}\boldsymbol{\sigma}\cdot\boldsymbol{n}\,dS = 0, \quad \text{and} \quad \boldsymbol{L}^H = \int_{S_p}\boldsymbol{r}\times\boldsymbol{\sigma}\cdot\boldsymbol{n}\,dS = 0, \tag{3}$$

where $\boldsymbol{n}$ is the outward unit normal to S_p, and $\boldsymbol{\sigma} = -p\boldsymbol{I} + \mu[\nabla\boldsymbol{v} + (\nabla\boldsymbol{v})^T]$ is the hydrodynamic stress tensor, in which $\boldsymbol{I}$ is the identity tensor and the superscript T denotes a transpose. The conditions Eqs. (3) signify that the "thrust" provided by the slip velocity is balanced by the "drag" due to particle translation. Therefore, the particle is *hydrodynamic* force-free in the thin-cloud limit; there is zero electric force on the effective surface enclosing the cloud and true particle surface, since together they have no net charge. (This statement does not hold in bounded or semibounded domains, such as electrophoresis near a wall, where a nonzero, dielectrophoretic type, electric force exists normal to the wall and must be balanced a net hydrodynamic force [19].) The situation is essentially different for a forced particle, where a net hydrodynamic force is required to balance the external body force, e.g., due to gravity for sedimentation.

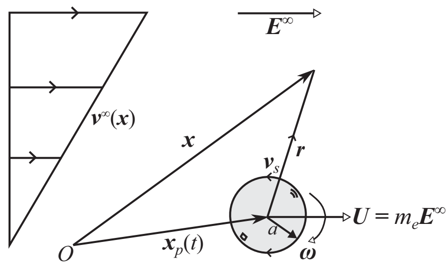

FIG. 2. Definition sketch for an electrophoretic particle in unbounded simple shear flow.

Smoluchowski solved Eqs. (1)–(3) for a spherical particle to obtain $\boldsymbol{U} = m_e \boldsymbol{E}^\infty$ and $\boldsymbol{\omega} = 0$, where $\boldsymbol{E}^\infty$ is the applied electric field. Morrison [25] proved that Smoluchowski's result is, in fact, valid for a particle of arbitrary shape provided that m_e is constant and polarization of the cloud is negligible [24]. Furthermore, Morrison [25] showed that the velocity field outside S_p is irrotational and decays like $1/r^3$ at large distances, as opposed to $1/r$ for a forced particle, which has implications for inertial cross-streamline migration. Consider a sphere (of radius a) moving along the streamlines of an unbounded simple shear flow, where U denotes its translational speed relative to the shear streamline passing through its center. Saffman [26] solved this problem for a forced particle using matched (i.e., inner-outer) asymptotic expansions at small Reynolds numbers, considering shear as the dominant mechanism for inertial screening of the velocity disturbance caused by the particle. Said screening occurs on the "Saffman length" $L_\mathrm{S} = (\mu/\rho\dot{\gamma})^{1/2} = a\mathrm{Re}_s^{-1/2}$, where ρ is the fluid density and $\dot{\gamma}$ is the shear rate, and $\mathrm{Re}_s = \rho\dot{\gamma}a^2/\mu$ is the Reynolds number of the shear. Therefore, the velocity disturbance is $O(Ua/L_\mathrm{S} = U\mathrm{Re}_s^{1/2})$ in the outer region beyond L_S, where inertial and viscous are comparable. This outer disturbance field forces a *singular* first inertial correction to the velocity field in the inner region (i.e., on the scale a) of $O(U\mathrm{Re}_s^{1/2})$, which yields a lift force of $O(\mu a U \mathrm{Re}_s^{1/2})$, to leading order. In contrast, the velocity disturbance due to an electrophoretic particle is $O(Ua^3/L_\mathrm{S}^3 = U\mathrm{Re}_s^{3/2})$ in the outer region, which means that the first inertial velocity field in the inner region is *regular* and $O(U\mathrm{Re}_s)$; hence, the leading-order lift force is $O(\mu a U \mathrm{Re}_s)$. This conclusion is valid for a particle of arbitrary shape; we calculate the leading-order lift for a sphere next.

III. ELECTROPHORETIC MIGRATION IN INERTIAL SHEAR FLOW

Consider an electrophoretic sphere in an ambient simple shear flow $\boldsymbol{v}^\infty(\boldsymbol{x}) = \boldsymbol{\Gamma}^\infty \cdot \boldsymbol{x}$, where $\boldsymbol{\Gamma}^\infty$ is the transpose of the constant velocity gradient tensor and $\boldsymbol{x}$ is the position vector from the origin O in a laboratory frame. Take Cartesian coordinates x, y, and z corresponding to the flow, gradient, and vorticity directions, respectively, for which $\boldsymbol{\Gamma}^\infty = \boldsymbol{S}^\infty + \boldsymbol{\Omega}^\infty$, where $\boldsymbol{S}^\infty = (\dot{\gamma}/2)(\boldsymbol{e}_x\boldsymbol{e}_y + \boldsymbol{e}_y\boldsymbol{e}_x)$ is the ambient rate of strain tensor, $\boldsymbol{\Omega}^\infty = (\dot{\gamma}/2)(\boldsymbol{e}_x\boldsymbol{e}_y - \boldsymbol{e}_y\boldsymbol{e}_x)$ is the transpose of the ambient vorticity tensor, and $\boldsymbol{e}_i$ denotes a Cartesian unit vector in the i direction. The sphere translates at velocity $\boldsymbol{U} = m_e\boldsymbol{E}^\infty$ and rotates at angular velocity $\boldsymbol{\omega}$. Figure 2 is a sketch of the problem for the case of particle translation along the streamlines of the shear, as relevant to the experiments discussed in Sec. I; however, our analysis below will be valid for an arbitrary direction of translation. The problem in the laboratory frame, with velocity field denoted by $\boldsymbol{v}$, is governed by the Navier-Stokes equations

$$\mu\nabla^2\boldsymbol{v} - \boldsymbol{\nabla}p = \rho\left(\frac{\partial\boldsymbol{v}}{\partial t} + \boldsymbol{v}\cdot\boldsymbol{\nabla}\boldsymbol{v}\right), \quad \boldsymbol{\nabla}\cdot\boldsymbol{v} = 0, \tag{4}$$

$$\boldsymbol{v} = \boldsymbol{U} + \boldsymbol{\omega}\times[\boldsymbol{x} - \boldsymbol{x}_p(t)] + \boldsymbol{v}_s \quad \text{on} \quad |\boldsymbol{x} - \boldsymbol{x}_p(t)| = a, \tag{5}$$

$$\boldsymbol{v} \to \boldsymbol{v}^\infty(\boldsymbol{x}) \quad \text{and} \quad p \to 0 \quad \text{as} \quad |\boldsymbol{x} - \boldsymbol{x}_p(t)| \to \infty, \tag{6}$$

where $\boldsymbol{x}_p(t)$ is the position of the particle centroid at time t, and $\boldsymbol{v}_s = \frac{3}{2}(\boldsymbol{nn} - \boldsymbol{I}) \cdot \boldsymbol{U}$ is the electro-osmotic slip velocity on the sphere [24]. We wish to calculate the hydrodynamic force $\boldsymbol{F}^H$ on the particle, the y component of which corresponds to a lift that would cause cross-streamline migration of an unconstrained particle. The angular velocity $\boldsymbol{\omega}$ is determined from the requirement that the particle is torque free.

We adopt a comoving frame translating with $\boldsymbol{U}$, in which the velocity field, denoted $\boldsymbol{u}$, is steady, and the flow at large distances approaches $-\boldsymbol{U} + \boldsymbol{\Gamma}^\infty \cdot \boldsymbol{r} + \boldsymbol{v}^\infty(0)$, where $\boldsymbol{r} = \boldsymbol{x} - \boldsymbol{x}_p(t)$. Here, $\boldsymbol{v}^\infty(0)$ is the velocity of the streamline through the centroid $\boldsymbol{r} = 0$; for unbounded simple shear one can take $\boldsymbol{v}^\infty(0) = 0$ without loss of generality. There exists a constant pressure gradient $-\rho\boldsymbol{\Gamma}^\infty \cdot \boldsymbol{U}$ in the comoving frame, to ensure that the far-field flow is a solution to the Navier-Stokes equations [27]. Hence, we define the disturbance velocity and pressure fields in the comoving frame as $\boldsymbol{u}' = \boldsymbol{u} - \boldsymbol{\Gamma}^\infty \cdot \boldsymbol{r} + \boldsymbol{U}$ and $p' = p + \rho\boldsymbol{r} \cdot \boldsymbol{\Gamma}^\infty \cdot \boldsymbol{U}$. The problem is cast in dimensionless form by normalizing distance by a; ambient velocity gradient and the angular velocity of the particle by $\dot{\gamma}$; electrokinetic slip velocity, particle translational velocity, and disturbance velocity field by $U = m_e E^\infty$, where $E^\infty = |\boldsymbol{E}^\infty|$; and pressure and stress by $\mu U/a$ (and thus force by $\mu U a$). The dimensionless disturbance problem reads

$$\nabla^2 \boldsymbol{u}' - \nabla p' = \mathrm{Re}_p(\boldsymbol{u}' \cdot \nabla \boldsymbol{u}' - \hat{\boldsymbol{U}} \cdot \nabla \boldsymbol{u}') + \mathrm{Re}_s[\boldsymbol{\Gamma}^\infty \cdot \boldsymbol{u}' + (\boldsymbol{\Gamma}^\infty \cdot \boldsymbol{r}) \cdot \nabla \boldsymbol{u}'], \quad \nabla \cdot \boldsymbol{u}' = 0, \tag{7}$$

$$\boldsymbol{u}' = Q(\boldsymbol{\omega} \times \boldsymbol{r} - \boldsymbol{\Gamma}^\infty \cdot \boldsymbol{r}) + \hat{\boldsymbol{U}} + \boldsymbol{u}_s \quad \text{on} \quad r = 1, \tag{8}$$

$$\boldsymbol{u}' \to 0 \ \text{ and } \ p' \to 0 \ \text{ as } \ r \to \infty, \tag{9}$$

where all variables in Eqs. (7)–(9) are dimensionless, and $\boldsymbol{u}_s = \frac{3}{2}(\boldsymbol{nn} - \boldsymbol{I}) \cdot \hat{\boldsymbol{U}}$ is the slip velocity, in which $\hat{\boldsymbol{U}}$ is a unit vector in the direction of particle translation. In Eqs. (7)–(9), $Q = \dot{\gamma}a/U$, and $\mathrm{Re}_p = \rho U a/\mu$ and $\mathrm{Re}_s = \rho\dot{\gamma}a^2/\mu$ are Reynolds numbers based on the electrophoretic velocity and ambient shear, respectively, both of which are small in experiments.

In Stokes flow ($\mathrm{Re}_p = \mathrm{Re}_s = 0$) the velocity field is a superposition of the flows due to the phoretic motion ($\boldsymbol{u}'_{0p}$, say) and the imposed shear ($Q\boldsymbol{u}'_{0s}$), which are [24,28]

$$\boldsymbol{u}'_{0p} = \frac{1}{2r^3}\left(3\frac{\boldsymbol{rr}}{r^2} - \boldsymbol{I}\right) \cdot \hat{\boldsymbol{U}}, \tag{10}$$

$$\boldsymbol{u}'_{0s} = -\frac{\boldsymbol{S}^\infty \cdot \boldsymbol{r}}{r^5} - \frac{5}{2r^3}\left(1 - \frac{1}{r^2}\right)\frac{(\boldsymbol{rr} : \boldsymbol{S}^\infty)\boldsymbol{r}}{r^2}. \tag{11}$$

There is no pressure field associated with the (irrotational) electrophoretic Stokes flow, $p'_{0p} = 0$; the shear generates a pressure Qp'_{0s}, where $p'_{0s} = -5\boldsymbol{rr} : \boldsymbol{S}^\infty/r^5$. The flows Eqs. (10) and (11) yield zero net force on the particle. The particle rotates at one-half of the vorticity of the ambient shear, $\boldsymbol{\omega}_0 = -\frac{1}{2}\boldsymbol{e}_z$. The electrophoretic flow is $O(\mathrm{Re}_s^{3/2})$ in the outer region $r = O(\mathrm{Re}_s^{-1/2})$, meaning that the first inertial correction to the inner region ($r = O(1)$) can be determined via the regular expansions

$$\boldsymbol{u}' = \boldsymbol{u}'_{0p} + Q\boldsymbol{u}'_{0s} + \mathrm{Re}_s Q\boldsymbol{u}'_{1s} + \mathrm{Re}_s \boldsymbol{u}'_{1l} + O\big(\mathrm{Re}_s^{3/2}\big), \tag{12}$$

$$p' = Qp'_{0s} + \mathrm{Re}_p p'_{1p} + \mathrm{Re}_s Q p'_{1s} + \mathrm{Re}_s p'_{1l} + O\big(\mathrm{Re}_s^{3/2}\big), \tag{13}$$

where the $O(\mathrm{Re}_s^{3/2})$ error arises from matching with the outer region. The velocity expansion Eq. (12) cannot contain terms solely dependent on Re_p, since the irrotational flow $\boldsymbol{u}'_{0p}$ is a solution to the Navier-Stokes equations with an inertial ("Bernoulli") pressure $\mathrm{Re}_p p'_{1p}$, where $p'_{1p} = -\frac{1}{2}[(\hat{\boldsymbol{U}} - \boldsymbol{u}'_{0p}) \cdot (\hat{\boldsymbol{U}} - \boldsymbol{u}'_{0p})]$. Since $\boldsymbol{u}'_{0p}$ is an even function of position $\boldsymbol{r}$, so too is p'_{1p}. Hence, this pressure distribution cannot generate a net force. Likewise, the $O(Q\mathrm{Re}_s)$ terms cannot generate lift, because they are only due to the shear flow around the particle. Thus, it is the $O(\mathrm{Re}_s)$ velocity and pressure fields that generate the leading-order lift force. Inserting Eqs. (12) and (13) into Eqs. (7)–(9) we find that these fields satisfy the inhomogeneous Stokes flow problem

$$\nabla^2 \boldsymbol{u}'_{1l} - \nabla p'_{1l} = \boldsymbol{f}'_{1l}, \quad \nabla \cdot \boldsymbol{u}'_{1l} = 0, \tag{14}$$

$$\boldsymbol{u}'_{1l} = \boldsymbol{\omega}_{1l} \times \boldsymbol{r} \ \text{ on } \ r = 1, \ \ \boldsymbol{u}'_{1l} \to 0 \ \text{ and } \ p'_{1l} \to 0 \ \text{ as } \ r \to \infty. \tag{15}$$

Here, $\boldsymbol{\omega}_{1l}$ is the $O(\mathrm{Re}_s)$ angular velocity of the particle, and the forcing

$$\boldsymbol{f}'_{1l} = \boldsymbol{u}'_{0s} \cdot \nabla \boldsymbol{u}'_{0p} + \boldsymbol{u}'_{0p} \cdot \nabla \boldsymbol{u}'_{0s} - \hat{\boldsymbol{U}} \cdot \nabla \boldsymbol{u}'_{0s} + \boldsymbol{\Gamma}^{\infty} \cdot \boldsymbol{u}'_{0p} + (\boldsymbol{\Gamma}^{\infty} \cdot \boldsymbol{r}) \cdot \nabla \boldsymbol{u}'_{0p}. \tag{16}$$

The far-field condition in Eq. (15) should be interpreted as the $O(\mathrm{Re}_s)$ inner velocity and pressure fields matching to a null outer solution at this order.

The $O(\mathrm{Re}_s)$ force on the particle is

$$\boldsymbol{F}^H_{1l} = \frac{4\pi}{3} \boldsymbol{\Gamma}^{\infty} \cdot \hat{\boldsymbol{U}} + \int_{r=1} \boldsymbol{\sigma}'_{1l} \cdot \boldsymbol{n} \, dS, \tag{17}$$

where the first term is due to the pressure gradient in the comoving frame, and $\boldsymbol{\sigma}'_{1l}$ is the $O(\mathrm{Re}_s)$ disturbance stress. To compute $\boldsymbol{F}^H_{1l}$ one could, in principle, first determine $\boldsymbol{\sigma}'_{1l}$ from the solution of Eqs. (14) and (15) and then perform the surface integral in Eq. (17). However, we can obviate this tedious calculation via the reciprocal theorem, which relates the $O(\mathrm{Re}_s)$ velocity and stress fields to those of an "auxiliary" Stokes flow in the same domain, with velocity $\tilde{\boldsymbol{u}}$ and stress $\tilde{\boldsymbol{\sigma}}$, via the integral identity

$$\int \boldsymbol{u}'_{1l} \cdot \tilde{\boldsymbol{\sigma}} \cdot \boldsymbol{n} \, dS + \int \boldsymbol{u}'_{1l} \cdot \tilde{\boldsymbol{f}} \, dV = \int \tilde{\boldsymbol{u}} \cdot \boldsymbol{\sigma}'_{1l} \cdot \boldsymbol{n} \, dS + \int \tilde{\boldsymbol{u}} \cdot \boldsymbol{f}'_{1l} \, dV, \tag{18}$$

where $\boldsymbol{f}'_{1l}$ Eq. (16) and $\tilde{\boldsymbol{f}}$ are the body force densities in each flow. The surface integrals in Eq. (18) are over the sphere and a "bounding" surface that encloses the fluid volume V. The auxiliary flow is chosen to be that due to a sphere translating at velocity $\tilde{\boldsymbol{V}}$ in the absence of a body force density ($\tilde{\boldsymbol{f}} = 0$), for which $\tilde{\boldsymbol{u}} = \boldsymbol{H} \cdot \tilde{\boldsymbol{V}}$, and $\tilde{\boldsymbol{\sigma}} \cdot \boldsymbol{n} = -\frac{3}{2}\tilde{\boldsymbol{V}}$ at $r = 1$, where [28]

$$\boldsymbol{H} = \frac{3}{4}\left(\frac{1}{r} + \frac{1}{3r^3}\right)\boldsymbol{I} + \frac{3}{4}\left(\frac{1}{r} - \frac{1}{r^3}\right)\frac{\boldsymbol{rr}}{r^2}. \tag{19}$$

It is readily shown that the integrals over the bounding surface vanish as the radius of that surface is taken to infinity. Thus, Eq. (18) returns

$$\int_{r=1} \boldsymbol{\sigma}'_{1l} \cdot \boldsymbol{n} \, dS = -\int \boldsymbol{H} \cdot \boldsymbol{f}'_{1l} \, dV. \tag{20}$$

Therefore, to compute $\boldsymbol{F}^H_{1l}$ now requires evaluation of a volume integral, whose integrand involves $\boldsymbol{H}$ and the known flows $\boldsymbol{u}'_{0p}$ Eq. (10) and $\boldsymbol{u}'_{0s}$ Eq. (11). The quantity $\boldsymbol{H} \cdot \boldsymbol{f}'_{1l}$ decays as $1/r^4$ at large distances; the integral is convergent. The volume integral is evaluated using the tensor algebra software recently developed in Ref. [29]; our code is provided in the Supplemental Material [30]. The final result is

$$\boldsymbol{F}^H_{1l} = \pi\left(\frac{8}{3}\boldsymbol{\Omega}^{\infty} - \frac{5}{6}\boldsymbol{S}^{\infty}\right) \cdot \hat{\boldsymbol{U}} = \frac{\pi}{4}\left(\frac{11}{6}\boldsymbol{e}_x\boldsymbol{e}_y - 7\boldsymbol{e}_y\boldsymbol{e}_x\right) \cdot \hat{\boldsymbol{U}}. \tag{21}$$

Evidently, the strain and rotation of the shear combine with the electrophoretic motion to generate lift. A discussion of Eq. (21) is deferred to Sec. V. One could also utilize the reciprocal theorem to calculate $\boldsymbol{\omega}_{1l}$, but that will not be pursued here: note that the value of $\boldsymbol{\omega}_{1l}$ does not affect the result Eq. (21), because the surface velocity at $O(\mathrm{Re}_s)$ is a solid-body rotation Eq. (15). This simplification does not occur for a body (phoretic or forced) with a mobile interface, such as a drop or a bubble, for which the surface velocity is not simply a solid-body rotation.

IV. ELECTROPHORETIC MIGRATION IN VISCOELASTIC SHEAR FLOW

Here, we calculate the migration of an electrophoretic particle in a weakly viscoelastic shear flow at zero Reynolds number. Our hypothesis is that the cross-streamline drift seen in recent experiments [17] is driven by normal stress differences, which are generically known to cause migration in the opposite direction to inertial forces. Those experiments used PEO solutions; typically, such polymeric liquids have a positive first normal stress coefficient Ψ_1, and a smaller, negative second normal stress coefficient Ψ_2. We model the polymer stress as a second-order fluid, which is a reasonable assumption as the channel Weissenberg number reported in Ref. [17] is less than unity. Therefore, the polymer stress is [4]

$$\boldsymbol{\sigma}^P = \Psi_1\left(\nabla \boldsymbol{v}^T \cdot \boldsymbol{S} + \boldsymbol{S}\cdot\nabla\boldsymbol{v} - \frac{\partial \boldsymbol{S}}{\partial t} - \boldsymbol{v}\cdot\nabla\boldsymbol{S}\right) + 4\Psi_2 \boldsymbol{S}\cdot\boldsymbol{S}. \tag{22}$$

The fluid flow in the laboratory frame again obeys Eqs. (4)–(6), except that the inertial terms in the momentum balance are replaced by $-\nabla\cdot\boldsymbol{\sigma}^P$. The problem is cast in dimensionless form using the normalizations in Sec. III. Therefore, the dimensionless momentum balance for the disturbance problem in the comoving frame is

$$\begin{aligned}\nabla^2\boldsymbol{u}' - \nabla p' = {} & \mathrm{Wi}_p \nabla\cdot[\boldsymbol{u}'\cdot\nabla\boldsymbol{S}' - \hat{\boldsymbol{U}}\cdot\nabla\boldsymbol{S}' - \boldsymbol{S}'\cdot\nabla\boldsymbol{u}' - (\nabla\boldsymbol{u}')^T\cdot\boldsymbol{S}' - \alpha\boldsymbol{S}'\cdot\boldsymbol{S}'] \\ & - \mathrm{Wi}_s\nabla\cdot[2\boldsymbol{S}^\infty\cdot\boldsymbol{S}' + 2\boldsymbol{S}'\cdot\boldsymbol{S}^\infty + \boldsymbol{S}'\cdot\boldsymbol{\Omega}^\infty - \boldsymbol{\Omega}^\infty\cdot\boldsymbol{S}' + \boldsymbol{S}^\infty\cdot\boldsymbol{\Omega}' - \boldsymbol{\Omega}'\cdot\boldsymbol{S}^\infty \\ & + (\boldsymbol{\Gamma}^\infty\cdot\boldsymbol{r})\cdot\nabla\boldsymbol{S}' + \alpha(\boldsymbol{S}'\cdot\boldsymbol{S}^\infty + \boldsymbol{S}^\infty\cdot\boldsymbol{S}')],\end{aligned} \tag{23}$$

where $\boldsymbol{S}'$ and $\boldsymbol{\Omega}'$ are the disturbance rate of strain and vorticity tensors. In Eq. (23), $\mathrm{Wi}_p = \Psi_1 U/\mu a$ and $\mathrm{Wi}_s = \Psi_1\dot{\gamma}/\mu$ are Weissenberg numbers based on the particle velocity and shear flow, respectively, and $\alpha = 4\Psi_2/\Psi_1$. The boundary conditions on Eq. (23) are, as before, Eqs. (8) and (9). We pose the expansions

$$\boldsymbol{u}' = \boldsymbol{u}'_{0p} + Q\boldsymbol{u}'_{0s} + \mathrm{Wi}_p\boldsymbol{u}'_{1p} + \mathrm{Wi}_s Q\boldsymbol{u}'_{1s} + \mathrm{Wi}_s\boldsymbol{u}'_{1l} + \cdots, \tag{24}$$

$$p' = Qp'_{0s} + \mathrm{Wi}_p p'_{1p} + \mathrm{Wi}_s Q p'_{1s} + \mathrm{Wi}_s p'_{1l} + \cdots, \tag{25}$$

in which the next higher-order terms are quadratic in Wi_s and Wi_p.

As in the inertial case, it is the $O(\mathrm{Wi}_s)$ velocity and pressure fields that generate the first contribution to the lift force, $\boldsymbol{F}^H_{1l} = \int_{r=1}\boldsymbol{\sigma}'_{1l}\cdot\boldsymbol{n}\,S$. These fields satisfy the inhomogeneous Stokes flow problem Eqs. (14) and (15), where $\boldsymbol{f}'_{1l}$ is now a "viscoelastic body force" given by $\boldsymbol{f}'_{1l} = -\nabla\cdot\boldsymbol{g}'_{1l}$, where

$$\begin{aligned}\boldsymbol{g}'_{1l} = {} & \hat{\boldsymbol{U}}\cdot\nabla\boldsymbol{S}'_{0s} - \boldsymbol{u}'_{0p}\cdot\nabla\boldsymbol{S}'_{0s} - \boldsymbol{u}'_{0s}\cdot\nabla\boldsymbol{S}'_{0p} + \boldsymbol{S}'_{0p}\cdot\nabla\boldsymbol{u}'_{0s} + \boldsymbol{S}'_{0s}\cdot\nabla\boldsymbol{u}'_{0p} + \left(\nabla\boldsymbol{u}'_{0p}\right)^T\cdot\boldsymbol{S}'_{0s} \\ & + \left(\nabla\boldsymbol{u}'_{0s}\right)^T\cdot\boldsymbol{S}'_{0p} + \alpha\left(\boldsymbol{S}'_{0p}\cdot\boldsymbol{S}'_{0s} + \boldsymbol{S}'_{0s}\cdot\boldsymbol{S}'_{0p}\right) + 2\boldsymbol{S}'_{0p}\cdot\boldsymbol{S}^\infty + 2\boldsymbol{S}^\infty\cdot\boldsymbol{S}'_{0p} + \boldsymbol{S}'_{0p}\cdot\boldsymbol{\Omega}^\infty \\ & - \boldsymbol{\Omega}^\infty\cdot\boldsymbol{S}'_{0p} - (\boldsymbol{\Gamma}^\infty\cdot\boldsymbol{r})\cdot\nabla\boldsymbol{S}'_{0p} + \alpha\left(\boldsymbol{S}'_{0p}\cdot\boldsymbol{S}^\infty + \boldsymbol{S}^\infty\cdot\boldsymbol{S}'_{0p}\right),\end{aligned} \tag{26}$$

where $\boldsymbol{S}'_{0s}$ and $\boldsymbol{S}'_{0p}$ denote the rate of strain tensors of the Stokes flows $\boldsymbol{u}'_{0s}$ and $\boldsymbol{u}'_{0p}$, respectively. Therefore, Eq. (20) can be used to evaluate the surface integral for $\boldsymbol{F}^H_{1l}$, with $\boldsymbol{f}'_{1l}$ determined from Eq. (26). Note that $\boldsymbol{H}\cdot\boldsymbol{f}'_{1l}$ now decays as $1/r^5$ at large distances. The volume integral in Eq. (20) is again evaluated on the computer [30], and the final result is

$$\boldsymbol{F}^H_{1l} = \frac{9\pi}{2}\left(1 - \frac{10}{3}\frac{\Psi_2}{\Psi_1}\right)\boldsymbol{S}^\infty\cdot\hat{\boldsymbol{U}} = \frac{9\pi}{4}\left(1 - \frac{10}{3}\frac{\Psi_2}{\Psi_1}\right)(\boldsymbol{e}_x\boldsymbol{e}_y + \boldsymbol{e}_y\boldsymbol{e}_x)\cdot\hat{\boldsymbol{U}}. \tag{27}$$

Only the straining component of the shear contributes to the lift force. This is in contrast to a forced particle, for which the lift force in a second-order fluid is dependent on the strain and rotation of the shear [7,8,10]. To verify Eq. (27), in the Appendix we provide an alternative computation of the lift force for a so-called "Weissenberg fluid" with $\Psi_2/\Psi_1 = -1/2$.

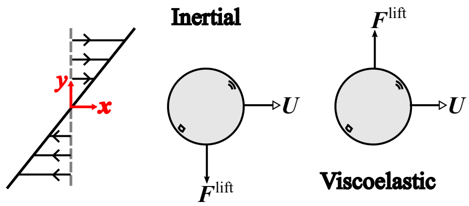

FIG. 3. Migration directions for an electrophoretic particle in inertial or viscoelastic shear.

V. COMPARISON TO EXPERIMENTAL OBSERVATIONS

We now compare the predictions from Secs. III and IV to experiments [12–17], focusing on those of Li and Xuan [17] who observed migration in Newtonian and polymeric liquids. We first discuss the Newtonian case. For particle motion along the shear flow, $\hat{\boldsymbol{U}} = \boldsymbol{e}_x$, Eq. (21) yields a *dimensional* leading-order lift force, say $\boldsymbol{F}^{\text{lift}}_{\text{inertial}}$, of

$$\boldsymbol{F}^{\text{lift}}_{\text{inertial}} \sim -\frac{7\pi}{4}\mu U a \text{Re}_s \boldsymbol{e}_y. \tag{28}$$

For $U > 0$ corresponding to electrophoresis along $+\boldsymbol{e}_x$, this force is directed along $-\boldsymbol{e}_y$, i.e., to shear streamlines that move opposite to the electrophoretic motion in a frame translating with the particle (Fig. 3). This is consistent with the experiments, which report migration to the channel walls when the electrophoretic velocity is in the same direction as the Poiseuille flow. Conversely, for $U < 0$ (28) predicts migration to streamlines moving with the particle, consistent with the observation of particle focusing to the channel center when the electrophoretic velocity opposes the Poiseuille flow. Further, substituting the definitions of U and Re_s into Eq. (28) yields the magnitude of the lift force

$$\left|\boldsymbol{F}^{\text{lift}}_{\text{inertial}}\right| \approx 5.50\frac{\varepsilon|\zeta|a^3\rho\dot{\gamma}E^\infty}{\mu}, \tag{29}$$

which corresponds to a migration speed

$$\left|\boldsymbol{U}^{\text{lift}}_{\text{inertial}}\right| = \frac{\left|\boldsymbol{F}^{\text{lift}}_{\text{inertial}}\right|}{6\pi\mu a} \approx 0.29\frac{\varepsilon|\zeta|a^2\rho\dot{\gamma}E^\infty}{\mu^2}. \tag{30}$$

Li and Xuan [17] used polystyrene spheres of $a = 5\,\mu$m in a Newtonian buffer whose properties we take as $\varepsilon = 7.08 \times 10^{-10}\,$F/m, $\mu = 10^{-3}\,$Pa s, and $\rho = 997\,$kg/m^3. The zeta potential of the particles was not reported, so we assume a typical value $\zeta = -50\,$mV. The channel has a rectangular cross section of width $w = 50\,\mu$m, depth $d = 100\,\mu$m and length $l = 2\,$cm, and sustains a volumetric flow rate $Q = 25\,\mu$l/h. Hence, following [17] we estimate the shear rate as $\dot{\gamma} = 2Q/(w^2d) = 55.6\,$/s. The electric field applied is $E^\infty = 300\,$V/cm. This yields from Eqs. (29) and (30) $|\boldsymbol{F}^{\text{lift}}_{\text{inertial}}| \approx 40.6\,$fN and $|\boldsymbol{U}^{\text{lift}}_{\text{inertial}}| \approx 0.42\,\mu$m/s. Hence, it takes a time $w/|\boldsymbol{U}^{\text{lift}}_{\text{inertial}}| \approx 118\,$s for a particle to migrate from the center of the channel to the wall. The residence time of a particle in the channel as it is convected along by the Poiseuille flow is $l/(Q/wd) \approx 15\,$s. Therefore a particle would migrate around 13% of the center-to-wall distance distance during its residence. The cross-stream distribution of particles is quite uniform at the start of the channel (see Fig. 3 in Ref. [17]); hence, this amount of migration would yield a modest accumulation of the total particle population to the walls. Nonetheless, these estimates, allied with our correct prediction of the lift direction, suggest that inertial forces are relevant to the migration in Newtonian liquids seen by Li and Xuan [17] and other studies [12–16].

Now we consider the viscoelastic case. For $\hat{\boldsymbol{U}} = \boldsymbol{e}_x$ Eq. (27) yields a *dimensional* leading-order lift force of

$$\boldsymbol{F}^{\text{lift}}_{\text{viscoelastic}} \sim \frac{9\pi}{4}\left(1 - \frac{10}{3}\frac{\Psi_2}{\Psi_1}\right)\mu U a \text{Wi}_s \boldsymbol{e}_y. \tag{31}$$

For $U > 0$ and if $\Psi_2/\Psi_1 < \frac{3}{10}$ the lift is toward streamlines moving in the direction of electrophoresis, which is consistent with the inward migration observed by Li and Xuan [17] in PEO solutions. Recall, in polymeric liquids Ψ_2 is negative and relatively small in magnitude compared to the positive Ψ_1; hence, the proviso $\Psi_2/\Psi_1 < \frac{3}{10}$ is reasonable. For $U < 0$ we predict migration to the walls, again in agreement with the experiments. Substituting the definitions of U and Wi_s into Eq. (31) yields the magnitude of the lift force

$$\left|\boldsymbol{F}^{\mathrm{lift}}_{\mathrm{viscoelastic}}\right| \approx 7.07\left(1 - 3.33\frac{\Psi_2}{\Psi_1}\right)\frac{\varepsilon|\zeta|a\Psi_1\dot{\gamma}E^{\infty}}{\mu}, \tag{32}$$

and migration speed

$$\left|\boldsymbol{U}^{\mathrm{lift}}_{\mathrm{viscoelastic}}\right| = \frac{\left|\boldsymbol{F}^{\mathrm{lift}}_{\mathrm{viscoelastic}}\right|}{6\pi\mu a} \approx 0.38\left(1 - 3.33\frac{\Psi_2}{\Psi_1}\right)\frac{\varepsilon|\zeta|\Psi_1\dot{\gamma}E^{\infty}}{\mu^2}, \tag{33}$$

which, interestingly, is independent of the particle size. Unfortunately, a value for Ψ_2 is not reported in Ref. [17]; we proceed simply by assuming $\Psi_2/\Psi_1 = 0$. Further, following Ref. [17] we take $\Psi_1 = 2\lambda\mu_p$ as predicted by the Oldroyd-B model in simple shear, in which the relaxation time $\lambda = 1.5\,\mathrm{ms}$ and polymer viscosity $\mu_p = 1.3 \times 10^{-3}\,\mathrm{Pa\,s}$. This value of μ_p is obtained as the difference of the zero shear viscosity for a 1000ppm PEO solution ($2.3 \times 10^{-3}\,\mathrm{Pa\,s}$) and a pure buffer solution ($1 \times 10^{-3}\,\mathrm{Pa\,s}$) reported in Refs. [17,31], respectively. Thus, $\Psi_1 = 3.9\,\mu\mathrm{Pa\,s}^2$. The flow rate $Q = 125\,\mu\mathrm{l/hr}$, which gives $\dot{\gamma} = 277.8/\mathrm{s}$. The electric field applied is again $E^{\infty} = 300\,\mathrm{V/cm}$. An electrophoretic mobility value of $1.2 \times 10^{-8}\,\mathrm{m^2/V\,s}$ was reported for these experiments; hence, we take the quantity $\varepsilon|\zeta|/\mu$ as equal to this value. Therefore, we estimate $|\boldsymbol{F}^{\mathrm{lift}}_{\mathrm{viscoelastic}}| \approx 13.8\,\mathrm{pN}$ and $|\boldsymbol{U}^{\mathrm{lift}}_{\mathrm{viscoelastic}}| \approx 63.6\,\mu\mathrm{m/s}$, which are much larger than in the inertial case. In fact, this migration speed would allow a particle to migrate essentially the entire center-to-wall distance during its residence in the microchannel. Therefore, it is plausible that the migration observed in Ref. [17] is due to viscoelastic forces arising from normal stress differences of the polymeric suspending fluid.

VI. DISCUSSION

The migration of an electrophoretic particle in a weakly inertial or viscoelastic simple shear flow has been analyzed. Predictions for the direction of cross-streamline lift of a particle that translates along the velocity axis of the shear are in agreement with recent experiments [12–17]. The estimated magnitudes of the lift forces further support the idea that the cumulative effect of weak instantaneous inertia or viscoelasticity is responsible, or at least contributes significantly, to the observed migration. Admittedly, our analysis has neglected factors that are likely important in the experiments, including particle-particle and particle-wall interactions (both hydrodynamic and electric); the nonuniform shear-rate of the Poiseuille flow; and the shape of the microchannel cross-section. Our simple calculation is therefore of quantitative value when: (i) the particle is not close to the wall; (ii) the particle volume fraction is small compared to unity, as in the experiments of Ref. [17], for example; (iii) the particle is not close to the center of the channel (where the shear rate vanishes); and (iv) the characteristic width of the cross-section is large compared to the particle radius (so that the flow is linear on the scale of the particle). Relaxing each of these restrictions deserves attention in future modeling work. Further experimental work could test the drift velocity scalings in Sec. V: namely, that the inertial drift velocity is proportional to a^2, while the viscoelastic drift velocity is independent of radius. The former scaling suggests that the combination of electrophoresis and inertial shear flow might be exploited for size-sensitive particle separation in microfluidic devices.

The above restrictions (i)–(iv) have, in fact, been partially relaxed in two recent articles from Choudhary *et al.* [32,33]. In the first [32], a rigid sphere undergoing electrophoresis in Poiseuille flow of a Newtonian fluid between infinite, planar, parallel walls was examined. The direction of electrophoresis is parallel to the streamlines of the ambient flow. The authors use the reciprocal theorem, following the procedure laid out by Ho and Leal [34], to calculate the cross-streamline force of the particle at small Reynolds number and for a small ratio of the particle radius to the gap between the walls. When the particle is sufficiently away from the walls and center of the flow, such that restrictions (i) and (iii) hold, they calculate a force equal to $-\frac{47}{80}\mu U a \mathrm{Re}_s \boldsymbol{e}_y$. Note, this result corresponds to Eq. (4.7) in their paper, which we have cast into our notation. The scaling, $O(Ua\mathrm{Re}_s)$, and direction of their lift force is consistent with our result Eq. (28); however, the coefficients, namely, $\frac{7\pi}{4}$ in our case and $\frac{47}{80}$ in theirs, are unequal. The reason for the difference is unclear. In the second paper [33], the same geometric setup is considered, but now the Poiseuille flow is of a second-order fluid at zero Reynolds number and small Weissenberg number. Equation (7) in that article gives an expression for the cross-streamline migration speed when wall effects are negligible. Additionally, if the curvature of the Poiseuille flow is ignored [corresponding to taking $\gamma = 0$ in their Eq. (7), or, equivalently, imposing restrictions (iii) and (iv)] their migration speed is given by $-\frac{1}{32\pi}(1 + \frac{2\Psi_2}{\Psi_1})U\mathrm{Wi}_s$. Again, we have cast this result into the present notation. The scaling of their migration speed, $O(U\mathrm{Wi}_s)$, is consistent with our result Eq. (33); however, the coefficients are unequal: i.e., we have a coefficient $\frac{3}{8}(1 - \frac{10\Psi_2}{3\Psi_1})$ compared to their $-\frac{1}{32\pi}(1 + \frac{2\Psi_2}{\Psi_1})$. Since $|\Psi_2/\Psi_1| \lesssim 0.1$ for most polymeric fluids [35], their migration direction is opposite to ours: that is, they predict a particle in a polymeric liquid to migrate to the center (walls) of a channel when its electrophoretic velocity is in the opposite (same) direction to (as) the flow. Their prediction is consistent with experiments presented in their article on 2.2-μm-diameter polystyrene spheres in a 250 ppm PEO solution. In contrast, Li and Xuan [17] observed migration of 10-μm-diameter polystyrene spheres in a 1000 ppm PEO solution in a direction consistent with our calculations. Here, it is worth reiterating that our result for the lift force for arbitrary Ψ_2/Ψ_1 (27) is consistent with an independent calculation for $\Psi_2/\Psi_1 = -1/2$ in the Appendix. Choudhary *et al.* [33] claim that the discrepancy between the two sets of experiments is due to additional viscoelastic effects, beyond the second-order fluid model, being operative at the larger polymer concentration. They suggest that a theoretical study of electrophoretic migration in viscoelastic shear using a constitutive equation with normal stress differences and shear thinning, e.g., Oldroyd-B or Giesekus, could shed light on the matter. This issue certainly deserves further attention.

We focused on electrophoresis along the direction of the shear flow, as relevant to the experiments that motivated the present study. However, our analysis is valid for an arbitrary direction of electrophoretic translation. For instance, for electrophoresis along the gradient of the shear, $\hat{\boldsymbol{U}} = \boldsymbol{e}_y$, the leading-order dimensional inertial force from (21) is $\boldsymbol{F}^{\mathrm{lift}}_{\mathrm{inertial}} \sim \frac{11\pi}{24}\mu U a \mathrm{Re}_s \boldsymbol{e}_x$, such that the sphere 'leads' the ambient shear streamline passing though its center by a velocity $\boldsymbol{F}^{\mathrm{lift}}_{\mathrm{inertial}}/6\pi\mu a \sim \frac{11}{144}U\mathrm{Re}_s\boldsymbol{e}_x$. In the viscoelastic case, from Eq. (27) the lead velocity is $\sim\frac{3}{8}(1 - \frac{10\Psi_2}{3\Psi_1})U\mathrm{Wi}_s\boldsymbol{e}_x$. To the present level of approximation, namely, from Eqs. (21) and (27), the motion of the sphere is unaffected for the "cross-shear flow" configuration in which electrophoresis occurs along the vorticity axis of the shear, $\hat{\boldsymbol{U}} = \boldsymbol{e}_z$. In the inertial case, the leading-order force on the particle should be $O(\mu U a \mathrm{Re}_s^{3/2})$ and, by symmetry, directed solely along $\boldsymbol{e}_z$, thereby modifying the velocity at which the sphere travels orthogonal to the plane of shear. This nonanalytic dependence originates from the leading-order velocity disturbance in the inertially dominated outer region far from the particle. An explicit calculation (i.e., to obtain the coefficient of the $O(\mu U a \mathrm{Re}_s^{3/2})$ term) would follow Saffman's approach [26], where the finite-sized sphere is replaced by a singular forcing in the outer region, in which the velocity disturbance is governed by an Oseen-type equation with shear as the dominant inertial effect. The essential difference is that for electrophoresis the forcing corresponds to a potential dipole, as opposed to a Stokeslet for Saffman's forced particle. In the viscoelastic case, Einarsson and Mehlig [10] have recently analyzed the motion of a forced sphere in an Oldroyd-B fluid at small Wi_s and Wi_p. (Note that our Wi_p is equivalent to twice their Deborah number De, and our Wi_s is equivalent to twice their Weissenberg number Wi.) For a cross-shear flow, their equation 68 shows that the leading-order modifications to the force on the particle are $O(\mu U a \mathrm{Wi}_s^2)$ and $O(\mu U a \mathrm{Wi}_s^2)$, again solely along $\boldsymbol{e}_z$. The same is expected for an electrophoretic particle; there can be no nonanalytic dependencies on Wi_s and Wi_p, since weak viscoelasticity is a regular perturbation, as opposed to the singular nature of weak inertia. However, given the lack of relevant experimental data for electrophoresis in inertial or viscoelastic cross-shear flow, we will not pursue detailed calculations here.

It is instructive to examine the differences between an electrophoretic and forced particle in terms of "lift tensors" for the migration of each. That is, from Eq. (21) the force on an electrophoretic particle in inertial shear flow can be written as $\boldsymbol{F}_{\mathrm{IP}} = -6\pi a\mu \boldsymbol{L}_{\mathrm{IP}} \cdot \boldsymbol{U}$, where the lift tensor

$$\boldsymbol{L}_{\mathrm{IP}} = \mathrm{Re}_s \begin{pmatrix} 0 & -\frac{11}{144} & 0 \\ \frac{7}{24} & 0 & 0 \\ 0 & 0 & 0 \end{pmatrix} \tag{34}$$

to leading order in Re_s, with an $O(\mathrm{Re}_s^{3/2})$ error. Here, the ij component of $\boldsymbol{L}_{\mathrm{IP}}$ gives the force in the i direction due to translation in the j direction. A forced particle in inertial shear is subject to a hydrodynamic force $\boldsymbol{F}_{\mathrm{IF}} = -6\pi \mu a(\boldsymbol{I} + \boldsymbol{L}_{\mathrm{IF}}) \cdot \boldsymbol{U}$, where

$$\boldsymbol{L}_{\mathrm{IF}} = \mathrm{Re}_s^{1/2} \begin{pmatrix} 0.0735 & 0.944 & 0 \\ 0.343 & 0.27 & 0 \\ 0 & 0 & 0.577 \end{pmatrix} \tag{35}$$

is the leading-order lift tensor, which is obtained from equation 5.28 of Ref. [36]. The main difference between the electrophoretic and forced particle is that the inertial lift force is $O(\mathrm{Re}_s^{-1/2})$ larger in the latter case. This occurs because of the longer-range velocity disturbance caused by a forced particle, which appears as a Stokeslet at large distances (a slow $1/r$ velocity decay), as opposed to the potential dipole disturbance due to an electrophoretic particle (a rapid $1/r^3$ decay). Mathematically, the $O(\mathrm{Re}_s^{1/2})$ inertial lift on a forced particle (35) originates from the flow in the inertially dominated outer region ($r = O(\mathrm{Re}_s^{-1/2})$), whereas (34) for an electro-phoretic particle arises due to weak inertial effects in the viscously dominated inner region ($r = O(1)$).

In a second-order fluid, the lift force on an electrophoretic particle is $\boldsymbol{F}_{\mathrm{VP}} = -6\pi \mu a \boldsymbol{L}_{\mathrm{VP}} \cdot \boldsymbol{U}$, where from Eq. (27)

$$\boldsymbol{L}_{\mathrm{VP}} = \frac{3}{8}\mathrm{Wi}_s\left(1 - \frac{10\Psi_2}{3\Psi_1}\right)\begin{pmatrix} 0 & -1 & 0 \\ -1 & 0 & 0 \\ 0 & 0 & 0 \end{pmatrix}. \tag{36}$$

In contrast, a forced particle in a second-order fluid is acted upon by a hydrodynamic force $\boldsymbol{F}_{\mathrm{VF}} = -6\pi \mu a(\boldsymbol{I} + \boldsymbol{L}_{\mathrm{VF}}) \cdot \boldsymbol{U}$, where

$$\boldsymbol{L}_{\mathrm{VF}} = \frac{1}{4}\mathrm{Wi}_s\left[\left(1 + \frac{2\Psi_2}{\Psi_1}\right)\begin{pmatrix} 0 & 1 & 0 \\ 1 & 0 & 0 \\ 0 & 0 & 0 \end{pmatrix} + \begin{pmatrix} 0 & 2 & 0 \\ -2 & 0 & 0 \\ 0 & 0 & 0 \end{pmatrix}\right]. \tag{37}$$

This expression for $\boldsymbol{L}_{\mathrm{VF}}$ is obtained from Eqs. (4.5a) and (4.5b) in Ref. [7] along with the errata to that article [8]. Here, the lift on an electrophoretic and forced particle is $O(\mathrm{Wi}_s)$ to leading order, originating from viscoelastic stresses on the scale of the particle $r = O(1)$. The lift tensor for an electrophoretic particle is symmetric, whereas the lift tensor for a forced particle is neither symmetric or antisymmetric. This is because only the strain of the ambient shear affects the lift on an electrophoretic particle, while the strain and rotation of the shear contribute to the lift on a forced particle. First, consider a forced particle moving along the streamlines of shear, $\hat{\boldsymbol{U}} = \boldsymbol{e}_x$. Equation (37) predicts that a lift force $\frac{3}{2}(1 - \frac{2\Psi_2}{\Psi_1})\pi \mu a U \mathrm{Wi}_s \boldsymbol{e}_y$ is exerted on the particle, which is in the same direction as an electrophoretic particle Eq. (31), since Ψ_2/Ψ_1 is negative for polymeric fluids. Second, consider a forced particle moving along the gradient axis of shear, $\hat{\boldsymbol{U}} = \boldsymbol{e}_y$. Equation (37) predicts that the particle translates relative to the shear streamline passing through its center at a velocity equal to $-\frac{3}{4}(1 + \frac{2\Psi_2}{3\Psi_1})U \mathrm{Wi}_s \boldsymbol{e}_x$. Given that $|\Psi_2/\Psi_1|$ is typically small compared to unity, the particle should therefore “lag” behind the ambient shear. In contrast, we have predicted above that an electrophoretic particle would ‘lead’ the ambient shear.

ACKNOWLEDGMENT

We acknowledge support from the Sharbaugh Presidential Fellowship to J.K.K.

APPENDIX: COMPUTATION OF THE VISCOELASTIC LIFT FORCE FOR $\Psi_2/\Psi_1 = -1/2$.

Here we compute the lift force on an electrophoretic sphere in shear flow of a second-order fluid for $\Psi_2/\Psi_1 = -1/2$, as a verification of Eq. (27). To that end, let p_N and $\boldsymbol{v}_N$ denote the (dimensional) pressure and velocity fields, respectively, belonging to an incompressible, Newtonian, zero-Reynolds-number flow. For $\Psi_2/\Psi_1 = -1/2$ the same velocity field along with a modified (“viscoelastic”) pressure, p_V, satisfy the zero-Reynolds-number flow of a second-order fluid, where

$$p_V = p_N - \frac{\Psi_1}{2\mu}\left(\frac{\partial}{\partial t} + \boldsymbol{v}\cdot\nabla\right)p_N - \frac{\Psi_1}{2}\boldsymbol{S}_N : \boldsymbol{S}_N, \tag{A1}$$

where $\boldsymbol{S}_N$ is the Newtonian rate of strain tensor [35]. Switching to a comoving frame and adopting the normalization scheme in Secs. III and IV, Eq. (A1) reads in dimensionless form

$$\begin{aligned} p'_V = p'_N &- \left(\tfrac{1}{2}\mathrm{Wi}_s\boldsymbol{\Gamma}^\infty\cdot\boldsymbol{r} - \tfrac{1}{2}\mathrm{Wi}_p\hat{\boldsymbol{U}} + \tfrac{1}{2}\boldsymbol{u}'_N\right)\cdot\nabla p'_N \\ &- \left[\tfrac{1}{2}\mathrm{Wi}_p\boldsymbol{S}'_N : \boldsymbol{S}'_N + \tfrac{1}{2}Q\boldsymbol{S}^\infty : \boldsymbol{S}^\infty + \tfrac{1}{2}\mathrm{Wi}_s\left(\boldsymbol{S}'_N : \boldsymbol{S}^\infty + \boldsymbol{S}^\infty_N : \boldsymbol{S}'_N\right)\right], \end{aligned} \tag{A2}$$

where all variables in Eq. (A2), and henceforth in this Appendix, are dimensionless. The Newtonian disturbance velocity and pressure fields are $\boldsymbol{u}'_N = \boldsymbol{u}'_{0p} + Q\boldsymbol{u}'_{0s}$ and $p'_N = Qp'_{0s}$, respectively. The viscoelastic pressure generates a force on the sphere given by

$$\boldsymbol{F}_V = -\int_{r=1} p'_V\boldsymbol{n}\,dS. \tag{A3}$$

Thus, only terms of p'_V that are odd in $\boldsymbol{r}$ contribute to $\boldsymbol{F}_V$; we denote these terms as $p_V'^{,\mathrm{lift}}$, and from the definitions of $\boldsymbol{u}'$ and p'_N we find

$$p_V'^{,\mathrm{lift}} = \tfrac{1}{2}\mathrm{Wi}_s\left[\left(\hat{\boldsymbol{U}} - \boldsymbol{u}'_{0p}\right)\cdot\nabla p_{0s} - \left(\boldsymbol{S}'_{0p} : \boldsymbol{S}'_{0s} + \boldsymbol{S}'_{0s} : \boldsymbol{S}'_{0p}\right) - \left(\boldsymbol{S}'_{0p} : \boldsymbol{S}^\infty + \boldsymbol{S}^\infty : \boldsymbol{S}'_{0p}\right)\right]. \tag{A4}$$

Hence, the force is

$$\boldsymbol{F}_V = -\int_{r=1} p_V'^{,\mathrm{lift}}\boldsymbol{n}\,dS = 12\pi\mathrm{Wi}_s\boldsymbol{S}^\infty\cdot\hat{\boldsymbol{U}}, \tag{A5}$$

where the last equality is obtained via evaluation of the surface integral on the computer [30]. The above result matches Eq. (27) for $\Psi_2/\Psi_1 = -1/2$.

[1] G. Segré and A. Silberberg, Radial particle displacements in Poiseuille flow of suspensions, Nature **189**, 209 (1961).

[2] G. Segré and A. Silberberg, Behaviour of macroscopic rigid spheres in Poiseuille flow Part 2. Experimental results and interpretation, J. Fluid Mech. **14**, 136 (1962).

[3] A. J. Hogg, The inertial migration of nonneutrally buoyant spherical particles in two-dimensional shear flows, J. Fluid Mech. **272**, 285 (1994).

[4] L. G. Leal, The motion of small particles in non-Newtonian fluids, J. Non-Newton Fluid Mech. **5**, 33 (1979).

[5] L. G. Leal, Particle motions in a viscous fluid, Annu. Rev. Fluid Mech. **12**, 435 (1980).

[6] B. P. Ho and L. G. Leal, Migration of rigid spheres in a two-dimensional unidirectional shear flow of a second-order fluid, J. Fluid Mech. **76**, 783 (1974).
[7] P. Brunn, The slow motion of a rigid particle in a second-order fluid, J. Fluid Mech. **82**, 529 (1977).
[8] P. Brunn, Errata to the slow motion of a sphere in a second-order fluid, Rheol. Acta **16**, 324 (1977).
[9] R. Vishnampet and D. Saintillan, Concentration instability of sedimenting spheres in a second-order fluid, Phys. Fluids **24**, 073302 (2012).
[10] J. Einarsson and B. Mehlig, Spherical particle sedimenting in weakly viscoelastic shear flow, Phys. Rev. Fluids **2**, 063301 (2017).
[11] A. M. Leshansky, A. Bransky, N. Korin, and U. Dinnar, Tunable Nonlinear Viscoelastic "Focusing" in a Microfluidic Device, Phys. Rev. Lett. **98**, 234501 (2007).
[12] Y. W. Kim and J. Y. Yoo, Axisymmetric flow focusing of particles in a single microchannel, Lab. Chip **9**, 1043 (2009).
[13] Y. M. Kim and J. Y. Yoo, Bidirectional inward migration of particles lagging behind a Poiseuille flow in a rectangular microchannel for 3D particle focusing, J. Micromech. Microeng. **25**, 027002 (2015).
[14] N. Cevheri and M. Yoda, Lift forces on colloidal particles in combined electroosmotic and poiseuille flow, Langmuir **30**, 13771 (2014).
[15] N. Cevheri and M. Yoda, Using shear and direct current electric fields to manipulate and self-assemble dielectric particles on microchannel walls, J. Nanotechnol. Eng. Med. **5**, 031009 (2014).
[16] D. Yuan, C. Pan, J. Zhang, S. Yan, Q. Zhao, G. Alici, and W. Li, Tunable particle focusing in a straight channel with symmetric semicircle obstacle arrays using electrophoresis-modified inertial effects, Micromachines **7**, 195 (2016).
[17] D. Li and X. Xuan, Electrophoretic slip-tuned particle migration in microchannel viscoelastic fluid flows, Phys. Rev. Fluids **3**, 074202 (2018).
[18] V. Lochab, A. Yee, M. Yoda, A. T. Conlisk, and S. Prakash, Dynamics of colloidal particles in microchannels under combined pressure and electric potential gradients, Microfluid. Nanofluid. **23**, 134 (2019).
[19] E. Yariv, "Force-free" electrophoresis? Phys. Fluids **18**, 031702 (2006).
[20] L. Liang, Y. Ai, J. Zhu, S. Qian, and X. Xuan, Wall-induced lateral migration in particle electrophoresis through a rectangular microchannel, J. Colloid Interface Sci. **347**, 142 (2010).
[21] S. Bike and D. Prieve, Electrokinetic lift of a sphere moving in slow shear flow parallel to a wall. II. Theory, J. Colloid Interface Sci. **175**, 422 (1995).
[22] O. Schnitzer, I. Frankel, and E. Yariv, Shear-induced electrokinetic lift at large Péclet numbers, Math. Model. Nat. Pheno. **7**, 64 (2012).
[23] D. Di Carlo, Inertial microfluidics, Lab Chip **9**, 3038 (2009).
[24] J. L. Anderson, Colloid transport by interfacial forces, Ann. Rev. Fluid Mech. **21**, 61 (1989).
[25] F. A. Morrison, Electrophoresis of a particle of arbitrary shape, J. Colloid Interface Sci. **34**, 210 (1970).
[26] P. G. Saffman, The lift on a small sphere in a slow shear flow, J. Fluid Mech. **22**, 385 (1965).
[27] E. Y. Harper and I-D. Chang, Maximum dissipation resulting from lift in a slow viscous shear flow, J. Fluid Mech. **33**, 209 (1968).
[28] L. G. Leal, *Advanced Transport Phenomena: Fluid Mechanics and Convective Transport Processes* (Cambridge University Press, Cambridge, UK, 2007).
[29] J. Einarsson, Computer algebra for microhydrodynamics, arXiv:1708.05788.
[30] See Supplemental Material at http://link.aps.org/supplemental/10.1103/PhysRevFluids.5.033702 for code to obtain Eqs. (21) and (27).
[31] X. Lu, S. Patel, M. Zhang, S. W. Joo, S. Qian, A. Ogale, and X. Xuan, An unexpected particle oscillation for electrophoresis in viscoelastic fluids through a microchannel constriction, Biomicrofluidics **8**, 021802 (2014).
[32] A. Choudhary, T. Renganathan, and S. Pushpavanam, Inertial migration of an electrophoretic rigid sphere in a two-dimensional Poiseuille flow, J. Fluid Mech. **874**, 856 (2019).

[33] A. Choudhary, D. Li, T. Renganathan, X. Xuan, and S. Pushpavanam, Electrokinetics enhances cross-stream particle migration in viscoelastic flows, arXiv:1907.03701.

[34] B. P. Ho and L. G. Leal, Inertial migration of rigid spheres in two-dimensional unidirectional flows, J. Fluid Mech. **65**, 365 (1974).

[35] R. B. Bird, R. C. Armstrong, and O. Hassager, *Dynamics of Polymeric Liquids Vol. 1* (Wiley, New York, 1987).

[36] K. Miyazaki, D. Bedeaux, and J. B. Avalos, Drag on a sphere in a slow shear flow, J. Fluid Mech. **296**, 373 (1995).